© 2014. Published by The Company of Biologists Ltd | The Journal of Experimental Biology (2014) 217, 2531-2539 doi:10.1242/jeb.103093

RESEARCH ARTICLE

Manipulation of BK channel expression is sufficient to alter auditory hair cell thresholds in larval zebrafish

Kevin N. Rohmann*,§, Joel A. Tripp§, Rachel M. Genova§,‡ and Andrew H. Bass¶

ABSTRACT

Non-mammalian vertebrates rely on electrical resonance for frequency tuning in auditory hair cells. A key component of the resonance exhibited by these cells is an outward calcium-activated potassium current that flows through large-conductance calcium-activated potassium (BK) channels. Previous work in midshipman fish (*Porichthys notatus*) has shown that BK expression correlates with seasonal changes in hearing sensitivity and that pharmacologically blocking these channels replicates the natural decreases in sensitivity during the winter non-reproductive season. To test the hypothesis that reducing BK channel function is sufficient to change auditory thresholds in fish, morpholino oligonucleotides (MOs) were used in larval zebrafish (*Danio rerio*) to alter expression of *slo1a* and *slo1b*, duplicate genes coding for the pore-forming α-subunits of BK channels. Following MO injection, microphonic potentials were recorded from the inner ear of larvae. Quantitative real-time PCR was then used to determine the MO effect on *slo1a* and *slo1b* expression in these same fish. Knockdown of either *slo1a* or *slo1b* resulted in disrupted gene expression and increased auditory thresholds across the same range of frequencies of natural auditory plasticity observed in midshipman. We conclude that interference with the normal expression of individual *slo1* genes is sufficient to increase auditory thresholds in zebrafish larvae and that changes in BK channel expression are a direct mechanism for regulation of peripheral hearing sensitivity among fishes.

KEY WORDS: Potassium channels, Auditory thresholds, Saccule, Hair cell

INTRODUCTION

The large-conductance calcium-activated potassium (BK) channel is essential for frequency tuning by electrical resonance in hair cells of non-mammalian vertebrates (Fettiplace and Fuchs, 1999). BK channel activation results from a combination of membrane depolarization and rises in internal calcium concentration through voltage-activated calcium channels (Fettiplace and Fuchs, 1999). Calcium-activated potassium currents have been observed in hair cells of the sacculus of fishes (Sugihara and Furukawa, 1989; Steinacker and Romero, 1992), the sacculus (Lewis and Hudspeth, 1983) and amphibian papilla (Pitchford and Ashmore, 1987) of frogs, and the cochlea of turtles (Crawford and Fettiplace, 1981), alligators (Fuchs and Evans, 1988), lizards (Eatock et al., 1993) and chicks (Fuchs et al., 1988). These currents play a key role in the frequency tuning of hair cells by contributing to membrane oscillations that set the characteristic frequency at which each cell is most sensitive (Fettiplace and Fuchs, 1999). A range of frequency sensitivity is accomplished through differences in the number of BK channels expressed in different hair cells (Fettiplace and Fuchs, 1999), as well as alternative splicing and modulation by the addition of β-subunits (Ramanathan et al., 1999).

In teleost fish, duplicate genes *slo1a* and *slo1b* code for the pore-forming α-subunits of BK channels (Rohmann et al., 2009). Recent studies of the plainfin midshipman fish (*Porichthys notatus*) support the hypothesis that BK channels play a predominant role in determining peripheral hearing sensitivity in fishes, as in non-mammalian tetrapods. Neurophysiological recordings from the hair cell epithelium of the saccule, the main auditory division of the inner ear of midshipman and many other fishes (Cohen and Winn, 1967; Popper and Fay, 1993), demonstrate seasonal shifts in the range of frequency encoding (Sisneros, 2009; Rohmann and Bass, 2011). Both males and females show about a 10 dB decrease in auditory thresholds that results in an enhanced range of frequency encoding when in reproductive condition. These seasonal changes can be experimentally replicated by manipulating BK function in the saccule: auditory thresholds increase when animals are treated with a specific BK channel antagonist (Rohmann et al., 2013). Quantitative real-time PCR (qPCR) also demonstrates a decrease in expression of both *slo1a* and *slo1b* mRNA transcripts in animals that display higher thresholds (Rohmann et al., 2013). Together, the evidence strongly supports the hypothesis that changes in BK channel expression are the principal mechanism underlying normal seasonal variation in hearing sensitivity. The current study extends these findings to zebrafish in order to more directly establish a role for BK channel function in the plasticity of auditory hair cell threshold.

Zebrafish, *Danio rerio* (Hamilton 1822), provide a tractable genetic model for the study of hearing (Nicolson, 2005). Among the tools available for genetic manipulation in zebrafish are morpholino oligonucleotides (MOs), short stable molecules that are injected into embryos and bind to RNA to knock down expression of a chosen gene (Moulton and Yan, 2008). Because of the role that BK channels play in hair cell frequency tuning among non-mammals, including seasonal hearing changes in midshipman, we hypothesized that reducing normal BK channel abundance by targeting expression of *slo1a* and *slo1b* would result in an increase in auditory thresholds in larval zebrafish. Saccular microphonic potentials were recorded in response to mechanical stimulation of the ear of animals treated with MOs to alter expression of *slo1a* and/or *slo1b*. As shown, MO injections directed at *slo1a* and *slo1b* resulted in increased auditory thresholds and modification of the expression of their target gene.

Department of Neurobiology and Behavior, Cornell University, Ithaca, New York, NY 14853, USA.
*Present address: Department of Otolaryngology, Head and Neck Surgery, Johns Hopkins University School of Medicine, Baltimore, MD 21205, USA. ‡Present address: University of Iowa Carver College of Medicine, Medical Scientist Training Program, Iowa City, IA 52242, USA.
§These authors contributed equally to this work

¶Author for correspondence (ahb3@cornell.edu)

Received 27 January 2014; Accepted 22 April 2014

The Journal of Experimental Biology (2014) doi:10.1242/jeb.103093

Table 1. Sequences of primers and morpholino oligonucleotides

Experiment	Target gene	Sequence
MO	*slo1a*	MO: 5′-GAGGAAAAGTGATTTTACCAGACCA-3′
		Control: 5′-GAGcAAAAcTcATTTTACgAgACCA-3′
	slo1b	MO: 5′-TCCACCTGAAAACAACAGCAGCAGC-3′
		Control: 5′-TCCACgTcAAAAgAACAcCAcCAGC-3′
MO verification	*slo1a*	F: 5′-GCTGGTGAACCTGTGTTCCATC-3′
		R: 5′-ACTTTCGAGCGTGATATGACCACAG-3′
	slo1b	F: 5′-TCGCAGCCTCTGTCGTAC-3′
		R: 5′-GAGACGCTCTCCAGTGTGATG-3′
qPCR	*slo1a* L	F: 5′-GCTGGTGAACCTGTGTTCCATC-3′
		R: 5′-ACGTCCCCATATCCCACCGT-3′
	slo1a S	F: 5′-GCTGGTGAACCTGTGTTCCATC-3′
		R: 5′-AGCTGGCAAACATGGCCGT-3′
	slo1b	F: 5′-GACACATCACACTGGAGAGCGTC-3′
		R: 5′-GTTGAGCACAGAGCCCTGGTAA-3′
	slo1b intron	F: 5′-CAGCCCAGTCACCAGACATC-3′
		R: 5′-GAGCTTGGAGGACTGCATCCAT-3′
	18S	F: 5′-AGAGGGACAAGTGGCGTTCAG-3′
		R: 5′-TCAAGCCCCAGTCCCAATCAC-3′

MO, morpholino oligonucleotide.

RESULTS

MO effects on *slo1* transcripts

To alter normal *slo1a* expression, a splice-blocking MO was designed and synthesized (Gene Tools, Philomath, OR, USA), targeting the exon–intron junction of zebrafish *slo1a* pre-mRNA (Table 1) at the 3′ end of exon 9 [Fig. 1A; exon numbering after Beisel et al. (Beisel et al., 2007)]. Splice-blocking MOs have the potential to produce a variety of aberrant splice products (Eisen and Smith, 2008). Possible products of our *slo1a* MO included, but are not limited to, either exon 9 removal or inclusion of the trailing intron. Exon 9 was targeted (Fig. 1A) because exclusion of this exon would result in removal of a major portion of the BK channel pore as well as the final transmembrane domain (Fig. 1B,C). Alternatively, intron inclusion would introduce a series of stop codons following exon 9, resulting in a greatly truncated protein. This aberrant splice product would lack the entire intracellular tail domain downstream of the pore and, consequently, both of the domains conferring calcium sensitivity (Fig. 1C).

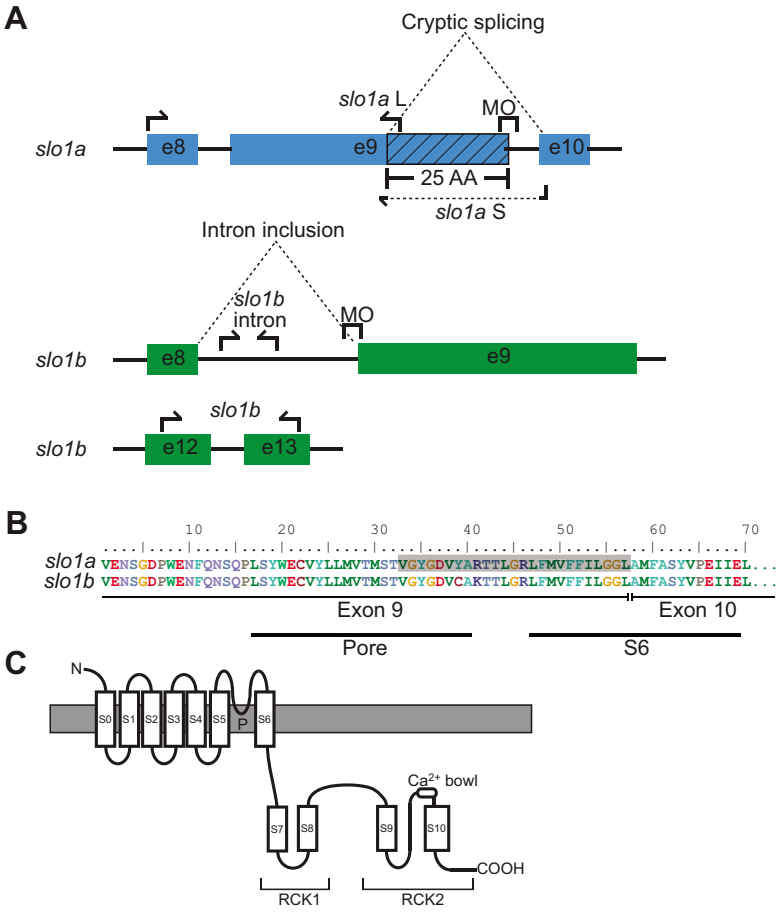

Fig. 1. *slo1a* and *slo1b* splice-blocking morpholino and qPCR design. (A) A splice-blocking morpholino (MO) was designed targeting exon 9 (e9) of *slo1a*. This MO causes activation of a cryptic splice site resulting in a truncation of the protein encoded by e9 by 25 amino acids (AA, hatched box). Primers (arrows) were designed to measure transcript abundance of both intact (L) and truncated (S) *slo1a* as well as *slo1b*. A splice-blocking MO was designed targeting exon 9 (e9) of *slo1b*. This MO caused inclusion of the intron between exons 8 and 9 resulting in the introduction of stop codons between e8 and e9, causing a loss of pore, S6 and intracellular C-terminal tail domains. (B) The 25 amino acid region of e9 removed by the *slo1a* MO corresponds to the final third (8 of 24 amino acids) of the BK channel pore and approximately the first half (11 of 23 amino acids) of the S6 transmembrane domain. Amino acid numbering is just for scale and does not reflect amino acid number within the entire BK channel protein. (C) Schematic diagram of the BK channel α-subunit encoded by each *slo1* gene.

The Journal of Experimental Biology

The Journal of Experimental Biology (2014) doi:10.1242/jeb.103093

To determine whether *slo1a* MO treatment resulted in exon exclusion (shortened PCR product) or intron inclusion (larger PCR product), PCR was conducted on whole-larva cDNA. PCR on *slo1a* MO-treated animals confirmed the production of a single aberrantly spliced *slo1a* transcript in addition to the normal *slo1a*. The splice-blocking *slo1a* MO targeted the exon–intron junction of the *slo1a* pre-mRNA at the 3′ end of exon 9, intending to exclude exon 9 or include the trailing intron containing stop codons. As is possible with splice-blocking MOs (Eisen and Smith, 2008), the MO caused activation of a cryptic splice site (Fig. 1A) that resulted in a 25 amino acid truncation of the protein encoded by exon 9 (Fig. 1B). Sequence analysis revealed that the 25 amino acid region corresponds to the final third (8 of 24 amino acids) of the BK channel pore and the first half (11 of 23 amino acids) of the S6 transmembrane domain (Fig. 1C). Importantly, the *slo1a* MO did not appear to alter *slo1b* splicing (data not shown), though we predict that its effect on *slo1a* processing results in non-functional products from this gene.

Similarly, to perturb normal *slo1b* expression, a splice-blocking MO was designed and synthesized targeting the intron–exon junction of *slo1b* pre-mRNA (Table 1) at the 5′ end of exon 9 and the 3′ end of the exon 8–exon 9 intron (Fig. 1A). In contrast to the single truncated transcript resulting from *slo1a* MO treatment, the *slo1b* MO caused intron inclusion between exons 8 and 9 by blocking the splice acceptor site at the 5′ end of exon 9 (Fig. 1A). The insertion of this 1026 base pair (bp) intron introduced several stop codons downstream of exon 8, including one as little as 13 amino acids downstream of exon 8. Thus, intron inclusion should produce a truncated protein missing the pore, calcium sensor and all other downstream residues (Fig. 1C).

Morphant behavioral phenotypes – MO dose–response profile

Initial testing began with establishing a dose–response profile using the *slo1a* MO. Dose–response studies are one way to examine the specificity of a MO effect on phenotype (Eisen and Smith, 2008). The initial doses tested were based on established dosing guidelines (Bill et al., 2009) as well as our own preliminary observations. Doses at or above 500 µmol l^{-1} (~5 ng/injection for *slo1a*) resulted in high rates of developmental defects (including small heads, shortened tails, curved bodies and impaired swimming) or death prior to the 3 days post-fertilization (dpf) physiology examination stage. These defects were likely caused by off-target effects often seen with high MO doses (Bedell et al., 2011).

We found good survival for a dose of 250 µmol l^{-1} and so conducted tests at this and lower doses until we failed to produce effects on the hair cell physiological phenotype (see below). At the 250 µmol l^{-1} dose, *slo1a* MO treatment resulted in a distinctive ‘circler’ phenotype characteristic of mutant zebrafish with hearing and balance deficits (Nicolson, 2005). Similar to these previously described mutants, a subset of *slo1a* MO-injected larvae swam in a circular motion when disturbed. However, because MO injections occurred at the one to two cell stage, motor deficits in *slo1a* MO-injected larvae could reflect cerebellar ataxia due to disruption of BK channel expression in the Purkinje cells of the cerebellum (Sausbier et al., 2004; Chen et al., 2010). Overall, 3 dpf *slo1a* MO-injected larvae formed three phenotypic groups: those appearing morphologically normal but displaying the circler behavior; those appearing morphologically and behaviorally normal; and those with severe developmental abnormalities, likely the result of mechanical damage from microinjection. Morphologically normal larvae with the circler phenotype, the most commonly observed, were selected for analysis. None of these behavioral effects were obvious for larvae treated at lower doses.

At an equivalent dose of 250 µmol l^{-1}, *slo1b* MO treatment did not result in any obvious locomotor or developmental phenotypes, aside from the minority with severe mechanically induced defects (see above). A complete dose–response analysis for the *slo1b* MO treatment was not conducted as we chose to use the same dose determined for *slo1a* MO in order to compare the relative effects of manipulating *slo1a* and *slo1b* transcripts at equal doses.

For the combined MO experiments, a dose of 125 µmol l^{-1} of each MO was used, so that the total concentration of the injected MO was 250 µmol l^{-1}. This dose was selected because, as with the *slo1a* MO, a total concentration of 500 µmol l^{-1} was either lethal or produced severe developmental defects (Bedell et al., 2011). At a total concentration of 250 µmol l^{-1}, the same three phenotypes were seen as in animals injected with 250 µmol l^{-1} *slo1a* MO. Again, larvae that were morphologically normal, but displayed the circler phenotype when disturbed were selected for physiology experiments.

Morphant hair cell physiology phenotypes

Our threshold data are reported as dB relative to the minimum stimulus output of our experimental apparatus (0.004 V from the lock-in amplifier), which produced responses equal to the ambient noise measured by the rig if either a dead fish or no fish was placed in the recording chamber. Wild-type animals at 3 dpf were recorded from throughout our studies to confirm that there were no changes in stimulus amplitude over time.

A glass recording microelectrode (2–20 MΩ) containing 3 mol l^{-1} KCl (Rohmann and Bass, 2011) was positioned medial to the posterior, saccular macula (Lu and DeSmidt, 2013) to record saccular microphonic potentials at 3 dpf from the otic vesicles of 13 non-manipulated wild-type, 24 *slo1a* MO-injected (total for three doses, see below), 12 *slo1a* mis-pair control MO-injected, 16 *slo1b* MO-injected and 16 *slo1b* mis-pair control-injected animals. Consistent with prior studies using similar stimulation and recording methods (Starr et al., 2004; Tanimoto et al., 2009; Lu and DeSmidt, 2013), and of behavioral audiograms (Bhandiwad et al., 2013), wild-type larvae were responsive to vibratory stimuli over the range of frequencies tested (175–500 Hz, Fig. 2). The two lowest *slo1a* MO

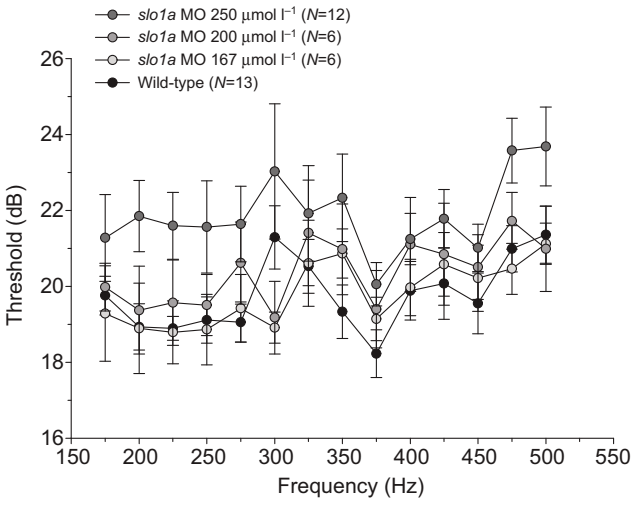

Fig. 2. *slo1a* MO causes a dose-dependent increase in auditory threshold. Only at the highest dose (250 µmol l^{-1}) does *slo1a* MO cause a change in auditory threshold compared with non-manipulated wild-type controls. Error bars indicate 95% confidence intervals.

The Journal of Experimental Biology (2014) doi:10.1242/jeb.103093

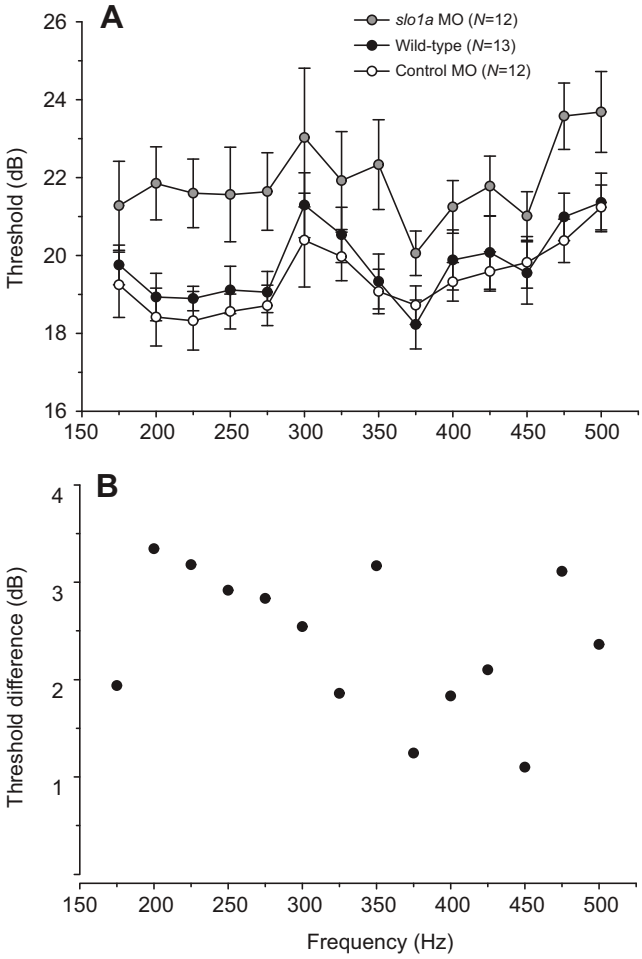

Fig. 3. *slo1a* MO increases auditory threshold. (A) Auditory hair cell thresholds were significantly increased by *slo1a* MO treatment compared with both control MO and non-manipulated wild-type controls. Error bars indicate 95% confidence intervals. (B) There is no significant relationship between frequency and difference in threshold between *slo1a* and control MO treatments.

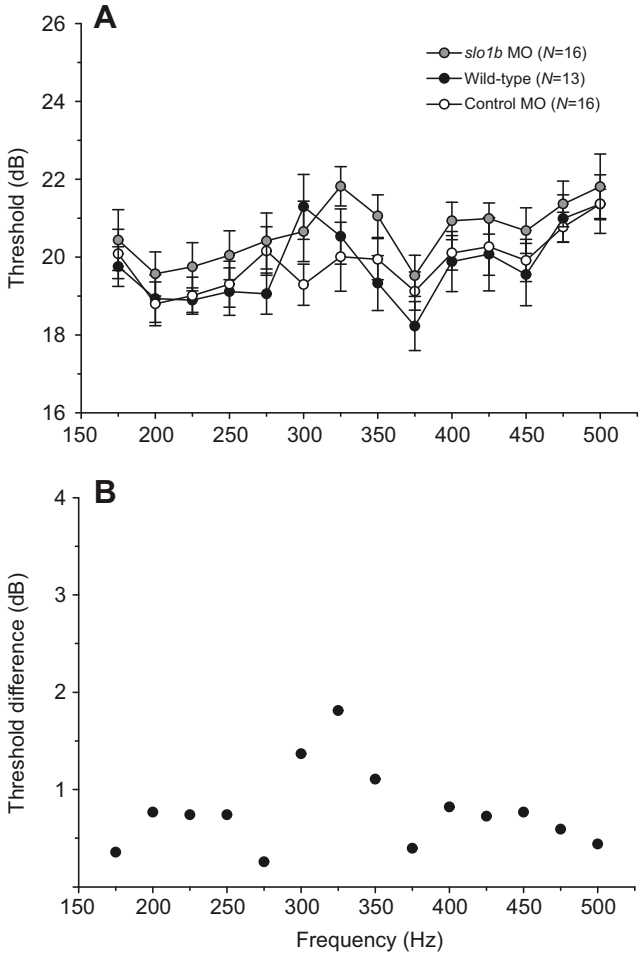

Fig. 4. *slo1b* MO increases auditory threshold. (A) Auditory hair cell thresholds were significantly increased by *slo1b* MO treatment compared with both control MO and non-manipulated wild-type animals. Error bars indicate 95% confidence intervals. (B) There is no significant relationship between frequency and difference in threshold between *slo1b* and control MO treatments.

concentrations tested, 167 µmol l^{-1} (Fig. 2; N=6 larvae; P=0.9066, Tukey HSD) and 200 µmol l^{-1} (Fig. 2; N=6; P=0.9066, Tukey HSD), were not sufficient to produce an auditory phenotype significantly different from that of un-manipulated wild-type control larvae. At the 250 µmol l^{-1} dose (N=12), *slo1a* MO treatment resulted in significant increases in hair cell threshold (Fig. 2; main effect P<0.0001 across all groups; P<0.0001, Tukey HSD).

There was an overall effect of *slo1a* MO treatment on auditory threshold (Fig. 3A; P<0.0001), with a significant interaction of frequency and treatment on threshold (P=0.0059). Thresholds of *slo1a* MO-injected individuals were significantly elevated compared with those of both *slo1a* control MO-injected (Fig. 3A; P<0.0001, Tukey HSD) and non-manipulated wild-type animals (Fig. 3A; P<0.0001, Tukey HSD). Thresholds did not differ between the *slo1a* control MO-injected and non-manipulated wild-type animals (Fig. 3A; P=0.99, Tukey HSD). Despite an interaction between frequency and main effect of treatment on threshold, there was no significant relationship between frequency and difference in threshold between *slo1a* and control MO treatments (Fig. 3B; P=0.20, R^2=0.13).

As with *slo1a* MO treatment, there was an overall effect of *slo1b* MO treatment on auditory threshold (Fig. 4A; P<0.0001), but no significant interaction of frequency and treatment on threshold (P=0.86). Thresholds of *slo1b* MO-injected individuals were significantly elevated compared with both lower *slo1b* control MO-injected (Fig. 4A; P=0.0266, Tukey HSD) and non-manipulated wild-type animals (P=0.0013, Tukey HSD). Thresholds did not differ significantly between the *slo1b* control MO-injected and non-manipulated wild-type animals (Fig. 4A; P=0.40, Tukey HSD). There was no significant relationship between frequency and difference in threshold between *slo1b* and control MO treatments (Fig. 4B; P=0.91, R^2=0.0011).

Potentials were next recorded from 13 *slo1a/slo1b* combined MO-injected animals, 12 combined control MO-injected animals and 10 un-manipulated wild-type animals. There was an overall effect of *slo1a/slo1b* combined MO treatment on auditory threshold (Fig. 5; P=0.0001), but no significant interaction of frequency and treatment on threshold (P=0.0953). Thresholds of combined MO-injected individuals (P<0.0001, Tukey HSD) and combined control-injected individuals (P=0.0110, Tukey HSD) were significantly raised compared with those of non-manipulated wild-type animals (Fig. 5). However, thresholds did not differ significantly between the combined MO-injected and combined control-injected animals (Fig. 5; P=0.1992).

The Journal of Experimental Biology (2014) doi:10.1242/jeb.103093

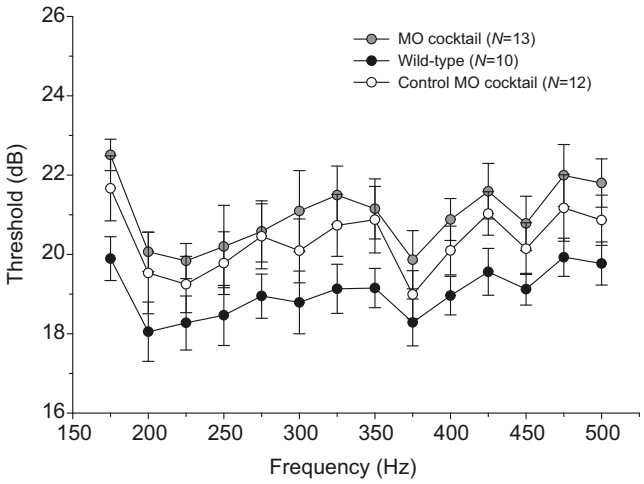

Fig. 5. *slo1a/slo1b* combined MO does not significantly increase auditory thresholds compared with control MO-injected animals. Both *slo1a/slo1b* MO- and *slo1a/slo1b* control-injected animals had auditory thresholds that were significantly higher than those of non-manipulated wild-type animals. Error bars indicate 95% confidence intervals.

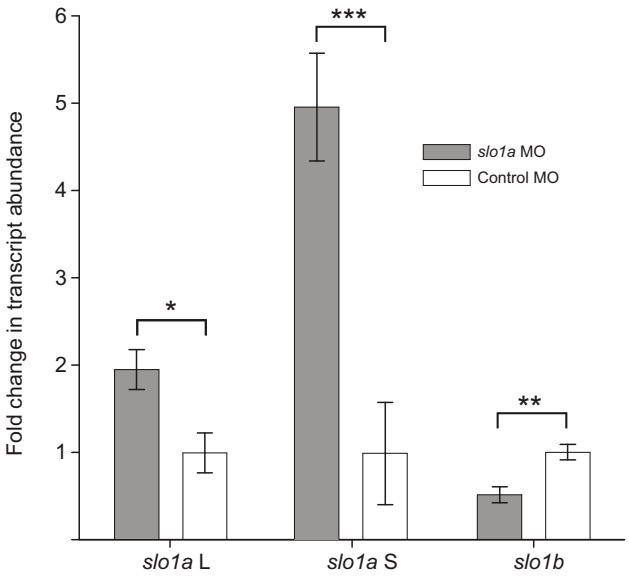

Fig. 6. *slo1a* MO treatment significantly alters *slo1* transcript abundance. *slo1a* MO treatment (*N*=10) caused significant increases in both MO-truncated *slo1a* (*slo1a* S) and intact *slo1a* (*slo1a* L) transcript abundance compared with control MO groups (*N*=9, *N*=10, respectively). *slo1a* MO treatment significantly decreased *slo1b* transcript abundance. **P*=0.0086, ***P*=0.0012, ****P*=0.0008. Error bars indicate standard errors.

qPCR

To directly correlate *slo1* transcript expression to individual physiological phenotype, we used qPCR to characterize the effects of MO treatment on *slo1* abundance in MO-injected (250 μmol l^{-1} dose) and control MO-injected animals from which hair cell thresholds were determined. To quantify a *slo1a* MO effect on *slo1a* and *slo1b* transcript levels, the abundance of *slo1b* and the MO-altered *slo1a* (*slo1a* S) and normal length *slo1a* (*slo1a* L) was determined from each *slo1a* control MO-injected (*N*=12) and *slo1a* MO-injected (*N*=11) animal. Sample sizes reported in figure legends report the actual successful qPCR samples analysed for each gene after exclusion of samples with signs of poor qPCR amplification due to poor RNA and cDNA sample such as amplification of 18s standards below the range of normal standard curve detection. As expected, *slo1a* MO treatment resulted in a significant increase of MO-truncated *slo1a* S transcript abundance compared with the control MO-treated group (Fig. 6; *P*=0.0008, Welch ANOVA). *slo1a* MO treatment also significantly increased intact *slo1a* L transcript abundance (Fig. 6; *P*=0.0086, Welch ANOVA). Conversely, *slo1a* MO treatment significantly decreased *slo1b* transcript abundance (Fig. 6; *P*=0.0012, ANOVA).

Of the three transcripts characterized, only MO-truncated *slo1a* S abundance significantly accounted for variability in auditory thresholds across both the *slo1a* MO- and *slo1a* control MO-treated animals (truncated *slo1a* S, *P*=0.0001; intact *slo1a* L, *P*=0.060; *slo1b*, *P*=0.75). However, no single transcript abundance accounted for significant threshold variability within treatment groups (truncated *slo1a* S, *P*=0.41; intact *slo1a* L, *P*=0.15; *slo1b*, *P*=0.45).

Similarly, qPCR was conducted on *slo1b* MO-injected and control MO-injected animals from which auditory thresholds were determined. To quantify *slo1b* MO effects on *slo1a* and *slo1b* transcript levels, the abundance of *slo1a* and of the aberrantly spliced *slo1b* (*slo1b* intron) and normal length *slo1b* was determined from each *slo1b* control MO-injected (*N*=16) and *slo1b* MO-injected animal (*N*=16). As expected, *slo1b* treatment significantly increased MO-altered *slo1b* intron transcripts, but also significantly increased *slo1a* and intact *slo1b* transcripts compared with the control MO-treated group (Fig. 7; all *P*<0.0001, ANOVA). However, no single transcript abundance accounted for variability in auditory thresholds across both the *slo1b* MO- and *slo1b* control MO-treated animals (*slo1a*, *P*=0.80; intact *slo1b*, *P*=0.45; *slo1b* intron, *P*=0.096) or for variability within treatment groups (*slo1a*, *P*=0.78; intact *slo1b*, *P*=0.35; *slo1b* intron, *P*=0.88).

Finally, to quantify combined *slo1a/slo1b* MO effects on *slo1a* and *slo1b* transcript levels, the abundance of *slo1a* L, *slo1a* S, *slo1b* and *slo1b* intron was determined from each *slo1a/slo1b* MO-injected (*N*=12), combined control MO-injected (*N*=6) and wild-type (*N*=9)

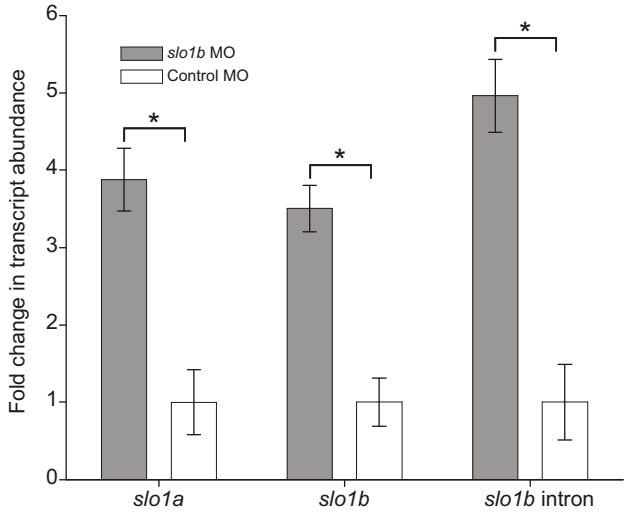

Fig. 7. *slo1b* MO treatment significantly alters *slo1* transcript abundance. *slo1b* MO treatment (*N*=16) caused significant increases in both total *slo1a* and total *slo1b* transcript abundance compared with the control MO group (*N*=15). *slo1b* MO treatment significantly increased the abundance of a *slo1b* transcript containing an intron inclusion between exons 8 and 9 (*slo1b* intron). **P*<0.0001 Welch ANOVA. Error bars indicate standard errors.

The Journal of Experimental Biology (2014) doi:10.1242/jeb.103093

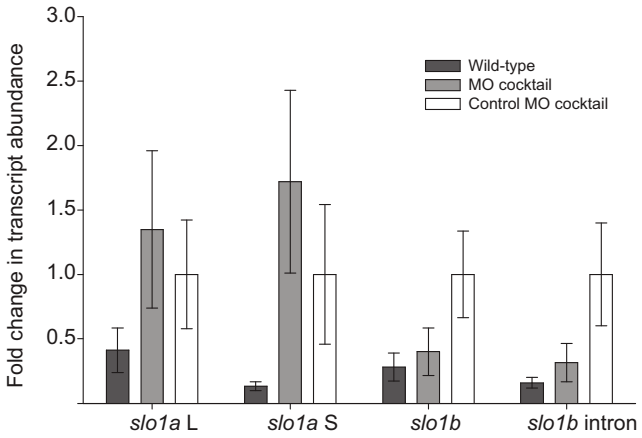

Fig. 8. *slo1a/slo1b* combined MO treatment does not significantly alter *slo1* transcript abundance. MO treatment (N=12) did not have a significant effect on the abundance of *slo1b*, *slo1b* transcript containing an intron inclusion (*slo1b* intron), intact *slo1a* (*slo1a* L) or MO-truncated *slo1a* (*slo1a* S) compared with control MO-injected (N=6) or wild-type (N=9) groups. Error bars indicate standard errors.

animal. The primer pairs used to quantify expression were the same as above. There were no significant differences in transcript abundance across all groups (Fig. 8) for intact *slo1a* L (P=0.0642), *slo1a* S (P=0.0558), intact *slo1b* (P=0.1014) or MO-altered *slo1b* intron (P=0.1061).

DISCUSSION

Microphonic potentials can be recorded from the saccule of developing zebrafish as young as 2 dpf (Tanimoto et al., 2009; Lu and DeSmidt, 2013) and are a valuable tool for determining the effect of mutations or MO treatments on auditory function (Lu and DeSmidt, 2013). Here, we used this larval zebrafish model to test the functional implications of manipulating the expression of BK channels encoded by two *slo1* genes on hair cell auditory thresholds. We previously identified *slo1* genes as playing a vital role in seasonal plasticity of inner ear (saccule) physiology in the plainfin midshipman (Rohmann et al., 2013), which is not as tractable to manipulations of gene expression as the zebrafish model. In this report, we show that interference with the normal expression of individual *slo1* genes is sufficient to increase auditory thresholds in zebrafish larvae and that changes in BK channel expression are a direct mechanism for regulation of peripheral hearing sensitivity among fishes.

Saccular microphonic potentials were recorded from the otic vesicles of zebrafish larvae at 3 dpf, a time point by which the auditory circuit is functional (Tanimoto et al., 2009). Although saccular auditory thresholds decrease over 3–7 dpf as the hair cell population increases in number (Lu and DeSmidt, 2013), we did not want to delay our recordings until a later time point because MOs are most effective up to 3 dpf (Bill et al., 2009). This limitation of MOs does not change our prediction of the disruptive effect of *slo1* MO treatment on hair cell function in zebrafish larvae in this initial investigation using this methodology.

Fish can detect auditory stimuli via particle motion and/or pressure (Popper and Fay, 2011). Following previous studies of hearing in larval zebrafish, a vibratory particle motion-dependent stimulus was used to stimulate the opening of mechanotransduction channels that lead to the encoding of auditory stimuli by hair cells in the inner ear (Starr et al., 2004; Tanimoto et al., 2009; Lu and DeSmidt, 2013). Particle motion is an appropriate stimulus for studying inner ear function at the 3 dpf time point we chose because the zebrafish inner ear is not yet capable of mature pressure detection until >56 dpf, when a connection to the swim bladder made through specialized bones known as the Weberian apparatus has fully developed and ossified (Grande and Young, 2004).

The current studies were an initial attempt to test our prior findings of BK channel-dependent natural plasticity in a zebrafish model system in which gene expression can be more readily manipulated. The particle motion generator used here did not allow for the calibration used in other studies (Lu and DeSmidt, 2013). However, because our experiment relies on relative differences in threshold between treatment groups, as in previous midshipman fish studies (Sisneros, 2009; Rohmann and Bass, 2011; Rohmann et al., 2013), it is not necessary to report thresholds relative to an absolute stimulus amplitude such as dB re. 1 nm of displacement. In future studies using this model system, piezo-electric actuators with nanometer precision calibration will be acquired and utilized in order to compare results between studies in our own and other laboratories.

When delivered individually, MOs designed to reduce expression of normal protein products of either *slo1a* or *slo1b* resulted in increased auditory thresholds in 3 dpf zebrafish larvae. Animals treated with *slo1a* MO had significantly higher auditory thresholds compared with those injected with a control MO, as well as un-manipulated wild-type animals. Animals treated with *slo1b* MO also showed increases in auditory threshold compared with control MO-injected and wild-type animals. This was expected, given the role of BK channels in electrical tuning of hair cells of fish and other non-mammalian vertebrates (Fettiplace and Fuchs, 1999) and previous work in midshipman fish showing that pharmacological blockage of BK channels in the saccule caused an increase in auditory thresholds (Rohmann et al., 2013). While the relative changes in threshold appear small (≤3 dB), they are within the behavioral discrimination range of other fishes including goldfish [2 dB (Fay, 1989)] and midshipman [3dB (McKibben and Bass, 1998)]. The results presented here provide direct evidence that changes in BK channel expression can serve as a mechanism for adjusting frequency sensitivity in the inner ear. The absolute changes in threshold were smaller than those observed in natural seasonal variation in midshipman, but likely reflect the limited effect of MOs on the zebrafish system due to homeostatic compensatory regulation of *slo1a* and *slo1b* expression (see below).

MO injection successfully manipulated expression of both *slo1a* and *slo1b*; however, these changes were not simply knockdowns of the targeted mRNA with corresponding increases in MO-altered products. Instead, treatment with either individual MO resulted in potentially compensatory changes in expression of both *slo1* genes. Animals that received the *slo1a* MO showed significantly higher expression of the MO-shortened version of *slo1a* and of the full-length *slo1a*, but also significantly less *slo1b*, than control MO-injected animals. In contrast, animals that were injected with the *slo1b* MO showed significant increases in expression of *slo1a*, as well as both normal and MO-altered *slo1b*. Thus, MO knockdown of one gene not only creates an altered version of the targeted transcript as predicted by MO design but also increases transcription of the normal version of the gene and affects expression of the other *slo1* gene. Compensatory homeostatic effects may explain the smaller increase in thresholds seen in *slo1b* MO-treated animals because *slo1b* MO caused upregulation of both *slo1* genes, while the *slo1a* MO caused increases of *slo1a* transcripts but decreases in *slo1b* transcripts. So, while BK channels are encoded by two *slo1*

The Journal of Experimental Biology (2014) doi:10.1242/jeb.103093

genes in teleost fish (Rohmann et al., 2009), they are not completely independent at a transcriptional level.

Another potential explanation for the differences in threshold changes for the *slo1a* and *slo1b* MOs is the relative effectiveness of each MO at the dose tested here. A dose–response experiment was carried out only for *slo1a*, and then the same concentration was used for the *slo1b* MO in order to test effects at the same dose. It is possible that any change in difference threshold, or in the pattern of gene expression, is due to differences in the efficacy of both MOs at the given dose. The fact that no morphological or locomotor phenotypes were seen in animals injected with the *slo1b* MO also suggests that this MO may not have as strong an effect at the same concentration. In spite of this, there was a significant effect of using either MO to manipulate expression changes. This effect may have been more robust and comparable to that of *slo1a* MO if a higher dose of *slo1b* MO had been tested.

In contrast to both individual MO treatments, animals injected with a combined *slo1a* and *slo1b* MO cocktail did not have significantly increased auditory thresholds compared with those injected with a combined control MO. However, both MO- and control-injected animals had higher thresholds compared with un-manipulated wild-type animals. Further, qPCR revealed that the combined MO did not have a significant effect on expression of normal or shortened *slo1a*, or normal or altered *slo1b*, when compared with either control-injected animals or un-manipulated wild-type animals. This was not expected, but there are at least two possible explanations for the result seen here. First, it is possible that although the total concentration of MO used in the combined MO experiment was the same as that in the individual MO experiments, the doses of each MO may have been too low to have an effect. That is, there may be some threshold for MO dose for these genes, below which that MO is not effective. This possibility is supported by the fact that in the dose–response experiment for *slo1a*, only the highest dose (250 µmol l^{-1}) had a significant effect on auditory thresholds. Ideally, the combined MO would have included 250 µmol l^{-1} of each individual MO, but this was not possible because of toxic effects at such a high dose. However, the explanation is not supported by the results of the physiology experiment using combined MO injection. Both the combined MO and the combined control caused significant increases of auditory threshold, so it is clear that MO injection had an effect in this case, but the effect may or may not have been directly related to knockdown of *slo1* genes. Another possible explanation for this result is off-target effects of the control MO. It is possible that while individual 5 bp mismatch MOs do not result in an impaired phenotype, when combined there is sufficient binding to non-target RNA to affect expression and produce an altered phenotype. This is consistent with the prediction that each additional MO added to an experimental mixture increases the chance of off-target effects (Eisen and Smith, 2008).

While MOs can be powerful tools to study the function of single genes, they have limitations, which can include off-target effects and toxicity at high doses; hence, it is extremely important to carefully control for these effects (Eisen and Smith, 2008; Bedell et al., 2011). These limitations are especially evident when attempting to use multiple MOs simultaneously, as toxicity may limit dosage below the threshold of effectiveness, and as stated above, use of multiple MOs in a mixture increases the chances of encountering off-target effects (Eisen and Smith, 2008). Further, manipulating gene expression may cause unintended effects on other genes that share a common regulatory network (Carvajal et al., 2001), such as duplicate *slo1* genes, and may drive compensatory changes in gene expression, which can counter the desired effect, as seen here in the individual MO experiments. In order to better understand the role of BK channels in hearing in this system, it may be necessary to take a different approach, such as combining MO use with strains of mutant animals.

In summary, our results build on those reported in midshipman fish. Pharmacological blocking of BK channels in midshipman results in increases of auditory threshold, with natural increases coinciding with decreases in expression of both *slo1a* and *slo1b* (Rohmann et al., 2013). MO injection in zebrafish larvae did not result in a direct knockdown of the targeted gene; however, manipulation of expression of individual *slo1* genes did result in increases in auditory thresholds. MOs were also successful at changing patterns of expression of both *slo1* genes, but did not necessarily act as simple knockdowns of the targeted gene. In contrast, simultaneous targeting of both *slo1a* and *slo1b* with a combined MO did not result in increased auditory thresholds over those of control MO-injected animals, and did not result in significant changes in expression of *slo1* genes. Future experiments are required in order to more definitively elucidate the potentially inter-dependent roles of *slo1a* and *slo1b* in determining peripheral auditory sensitivity.

MATERIALS AND METHODS

Animals

All experiments were conducted using wild-type zebrafish (*D. rerio*) embryos and larvae maintained in aquaria in accordance with Cornell University's Institutional Animal Care and Use Committee.

MOs

Two splice-blocking MOs were designed and synthesized (Table 1). The first targeted the exon–intron junction of zebrafish *slo1a* pre-mRNA at the 3′ end of exon 9 (Fig. 1A) and the second targeted the intron–exon junction of *slo1b* pre-mRNA at the 5′ end of exon 9 and the 3′ end of the exon 8–exon 9 intron (Fig. 1A). For each MO, a mis-pair control MO was designed with five mismatches (Table 1) to determine sequence specificity as well as off-target effects (Eisen and Smith, 2008).

All MOs were solubilized at a concentration of 1 mmol l^{-1} in UltraPure water (Life Technologies, Carlsbad, CA, USA). The resulting stocks were diluted to a working concentration of 250 µmol l^{-1} following preliminary dose–response tests (see Results). Developing blastulae with one to two cells were injected with 1.5625 nl of the diluted MO from a calibrated pressure injection device, delivering a final dose of 3.33 ng of MO targeting *slo1a* or *slo1b* alone, or combined *slo1a* and *slo1b* at equal concentration per embryo. This dose was chosen based on a dose–response curve for the *slo1a* MO (see Results).

MO verification

RNA was extracted from individual whole larva using Trizol (Invitrogen, Carlsbad, CA, USA), treated with DNase I (Invitrogen) to remove genomic DNA, and reverse translated using Superscript III Reverse Transcriptase (Invitrogen) following the manufacturer's protocols. Primers were designed (Table 1) from the zebrafish *slo1a* (Ensembl no. ENSDARG00000079840) and *slo1b* (Ensembl no. ENSDARG00000060237) sequences to determine the effects of *slo1a* and *slo1b* MO treatment. Amplification was performed with the FailSafe PCR System (Epicentre, Madison, WI, USA) with the following cycles: stage 1 – 94°C initial denaturation for 4 min; stage 2 – 94°C for 30 s, 57°C for 30 s, 72°C for 1 min (35 cycles); stage 3 – 72°C final extension for 10 min. The expected products were verified on a 1% agarose gel and sequenced by the Cornell University Life Sciences Core Laboratory Center to ensure proper sequence amplification.

Hair cell physiology

Following paralysis in 20 µl of 1 mg ml^{-1} α-bungarotoxin (Life Technologies) in Hank's solution, an individual larva was transferred to a recording dish, embedded with its right side facing up in 1% agarose in Hank's solution, and covered in Hank's solution containing 0.0002%

Methylene Blue (Westerfield, 2007; McLean et al., 2008). The recording platform rested upon a vibration isolation table inside a soundproof chamber (Industrial Acoustics, New York, NY, USA) with all equipment used for stimulation and recording of microphonic responses located outside the chamber. All recordings were at room temperature (20–23°C).

Under a dissecting microscope a metal stimulating rod with a 30 µm diameter tip was positioned at the posterior edge of the right otic vesicle along the posterior edge of the posterior otolith. The same stimulating rod was used in all experiments and kept at the same angle, making placement of the stimulus probe consistent between preparations. Vibratory stimuli were generated by the reference signal of an SR830 lock-in amplifier (SR830, Stanford Research Systems, Sunnyvale, CA, USA) driving a piezoelectric actuator (Piezosystem Jena, Jena, Germany). Custom-written MATLAB (MathWorks, Inc., Natick, MA, USA) software modified from that used in Rohmann and Bass (Rohmann and Bass, 2011) was used to control stimulus generation and data acquisition through the lock-in amplifier. Stimuli consisted of 500 ms bursts played at 1.5 s intervals repeated eight times. Stimuli were presented in 25 Hz increments from 175 to 500 Hz in random order.

Microphonic potentials were recorded with methods adapted for zebrafish larvae from studies of the sacculus of midshipman (Rohmann and Bass, 2011). A glass recording microelectrode (2–20 MΩ) containing 3 mol l^{-1} KCl was positioned medial to the posterior (saccular) macula (Nicolson, 2005). The electrode tip was positioned in the center of both the dorsal–ventral and rostral–caudal axes of the otolith. Briefly, microphonic potentials were amplified (Model 5A, Getting Instruments, San Diego, CA, USA), high-pass filtered and further amplified (SR650, Stanford Research Systems), and fed into the lock-in amplifier for analog to digital conversion and signal processing, and stored on a PC. From each larval zebrafish, a single threshold tuning curve was constructed using previous methods (Rohmann and Bass, 2011). Stimuli were presented eight times at each frequency with frequency order randomized. The amplitude was increased across frequencies until the mean of the eight responses at a given frequency was greater than two standard deviations above the mean background noise as measured under normal stimulus conditions but with power to the stimulus probe set to its minimum. Following completion of each threshold tuning curve, each larva was removed from the agarose mounting medium, flash frozen in liquid nitrogen, and stored at −80°C for later RNA extraction.

qPCR

Absolute qPCR was conducted on cDNA using gene-specific primer pairs designed from the nucleotide sequence of the zebrafish genes (Table 1). qPCR reactions were run in triplicate for each target gene along with no-template controls. The results of each triplicate set were averaged. Each reaction contained the following: 10 µl of 2× Power SYBR Green PCR Master Mix (Applied Biosystems, Foster City, CA, USA), 2 µl each of forward and reverse primers at a concentration of 100 nmol l^{-1}, 4 µl of H_2O and 2 µl of the appropriate cDNA. Reactions were run on an Applied Biosystems ViiA 7 System at the Cornell University Life Sciences Core Laboratory Center under the default manufacturer's conditions using 57°C as an annealing temperature. Gene copy number was determined using standard curve analysis for each target (Arterbery et al., 2010), including 18S rRNA (GenBank accession no. FJ915075.1), which was used as the reference gene for normalizing gene copy number. As briefly noted in the Results, qPCR sample sizes were sometimes smaller than physiology sample sizes because of the occasional poor RNA extraction yield as measured by the NanoDrop spectrophotometer (NanoDrop, Wilmington, DE, USA) or poor cDNA amplification as measured by low 18S rRNA copy number. Only standard curves with coefficients of determination (R^2) no less than 0.96 were used. Briefly, the raw C_t values were converted to copy number with the standard curve produced by the ViiA 7 software. The standards covered a linear range of 160–5e7 copies μl^{-1} of template for the *slo1a* MO qPCR plate, 32–2.5e6 copies μl^{-1} for the *slo1b* MO qPCR plates and 160–5e7 copies μl^{-1} for the combined MO plates. Each target gene copy number was normalized separately to the 18S copy number from the same individual. The normalized values were determined for each individual and fold expression change was calculated for each individual as the normalized value divided by the mean normalized MO control value. Initially, all qPCR products were verified on a 1% agarose gel and sequenced by the Cornell University Life Sciences Core Laboratory Center to ensure proper sequence amplification.

Statistics

All statistical analyses were performed using JMP 10 pro (SAS Institute Inc., Cary, NC, USA). Physiology data were analyzed as described previously (Rohmann and Bass, 2011; Rohmann et al., 2013). Briefly, the effect of MO treatment on thresholds was determined by a multilevel, repeated measures statistical model with MO treatment as the between-subject factor. Threshold was a response variable of each stimulus frequency. All responses across frequencies for a given set of recordings were nested within an individual fish. For analyses with more than two groups (e.g. comparison of multiple MO doses with control MO and non-injected control groups), Tukey–Kramer HSD *post hoc* tests were used to test for differences between pairs of groups. The relationship between change in threshold and frequency was tested using simple regression. All threshold data were graphed as means with 95% confidence interval error bars. qPCR data for *slo1a* or *slo1b* MO groups were analyzed with an ANOVA as described previously (Arterbery et al., 2010). Because qPCR reactions were carried out across several plates with an even number of each treatment group represented on each plate, qPCR data for the combined MO groups were fitted to a model with 18S-normalized expression as the response, and plate and treatment group as fixed effects. Data were graphed as means with error bars indicating standard errors. Where qPCR data and physiological measures were combined, qPCR data were incorporated into the physiological statistical model with gene expression either replacing MO treatment as the between-subject variable (within MO treatment group analyses) or in addition to MO treatment group (across MO treatment group analyses).

Acknowledgements

We especially thank J. R. Fetcho and his staff for providing the zebrafish and A. J. Hudspeth and Z. Lu for advice on the piezoelectric device and electrodes for inner ear stimulation; and J. V. DiPietro, D. J. Fergus, N. McGuire, J. C. Olthoff, J. E. Shea and J. Barry of the Cornell University Statistical Consulting Unit for technical assistance. We thank two anonymous reviewers for comments that improved the manuscript.

Competing interests

The authors declare no competing financial interests.

Author contributions

K.N.R. and A.H.B. designed the experiments; K.N.R., J.A.T. and R.M.G. conducted the experiments; K.N.R. and R.M.G. designed the morpholino oligonucleotide and qPCR strategy; K.N.R., J.A.T., R.M.G. and A.H.B. analyzed the data and wrote the paper.

Funding

This research was supported by a research grant from the National Institutes of Health [DC00092, A.H.B.] and a Cornell Graduate Fellowship (J.A.T.). Deposited in PMC for release after 12 months.

References

Arterbery, A. S., Deitcher, D. L. and Bass, A. H. (2010). Corticosteroid receptor expression in a teleost fish that displays alternative male reproductive tactics. *Gen. Comp. Endocrinol.* **165**, 83-90.

Bedell, V. M., Westcot, S. E. and Ekker, S. C. (2011). Lessons from morpholino-based screening in zebrafish. *Brief. Funct. Genomics* **10**, 181-188.

Beisel, K. W., Rocha-Sanchez, S. M., Ziegenbein, S. J., Morris, K. A., Kai, C., Kawai, J., Carninci, P., Hayashizaki, Y. and Davis, R. L. (2007). Diversity of Ca^{2+}-activated K^+ channel transcripts in inner ear hair cells. *Gene* **386**, 11-23.

Bhandiwad, A. A., Zeddies, D. G., Raible, D. W., Rubel, E. W. and Sisneros, J. A. (2013). Auditory sensitivity of larval zebrafish (*Danio rerio*) measured using a behavioral prepulse inhibition assay. *J. Exp. Biol.* **216**, 3504-3513.

Bill, B. R., Petzold, A. M., Clark, K. J., Schimmenti, L. A. and Ekker, S. C. (2009). A primer for morpholino use in zebrafish. *Zebrafish* **6**, 69-77.

Carvajal, J. J., Cox, D., Summerbell, D. and Rigby, P. W. (2001). A BAC transgenic analysis of the Mrf4/Myf5 locus reveals interdigitated elements that control activation and maintenance of gene expression during muscle development. *Development* **128**, 1857-1868.

Chen, X., Kovalchuk, Y., Adelsberger, H., Henning, H. A., Sausbier, M., Wietzorrek, G., Ruth, P., Yarom, Y. and Konnerth, A. (2010). Disruption of the olivo-cerebellar circuit by Purkinje neuron-specific ablation of BK channels. *Proc. Natl. Acad. Sci. USA* **107**, 12323-12328.

Cohen, M. J. and Winn, H. E. (1967). Electrophysiological observations on hearing and sound production in the fish, *Porichthys notatus*. *J. Exp. Zool.* **165**, 355-369.
Crawford, A. C. and Fettiplace, R. (1981). An electrical tuning mechanism in turtle cochlear hair cells. *J. Physiol.* **312**, 377-412.
Eatock, R. A., Saeki, M. and Hutzler, M. J. (1993). Electrical resonance of isolated hair cells does not account for acoustic tuning in the free-standing region of the alligator lizard's cochlea. *J. Neurosci.* **13**, 1767-1783.
Eisen, J. S. and Smith, J. C. (2008). Controlling morpholino experiments: don't stop making antisense. *Development* **135**, 1735-1743.
Fay, R. R. (1989). Intensity discrimination of pulsed tones by the goldfish (*Carassius auratus*). *J. Acoust. Soc. Am.* **85**, 500-502.
Fettiplace, R. and Fuchs, P. A. (1999). Mechanisms of hair cell tuning. *Annu. Rev. Physiol.* **61**, 809-834.
Fuchs, P. A. and Evans, M. G. (1988). Voltage oscillations and ionic conductances in hair cells isolated from the alligator cochlea. *J. Comp. Physiol. A* **164**, 151-163.
Fuchs, P. A., Nagai, T. and Evans, M. G. (1988). Electrical tuning in hair cells isolated from the chick cochlea. *J. Neurosci.* **8**, 2460-2467.
Grande, T. and Young, B. (2004). The ontogeny and homology of the Weberian apparatus in the zebrafish *Danio rerio* (Ostariophysi: Cypriniformes). *Zool. J. Linn. Soc.* **140**, 241-254.
Lewis, R. S. and Hudspeth, A. J. (1983). Voltage- and ion-dependent conductances in solitary vertebrate hair cells. *Nature* **304**, 538-541.
Lu, Z. and DeSmidt, A. A. (2013). Early development of hearing in zebrafish. *J. Assoc. Res. Otolaryngol.* **14**, 509-521.
McKibben, J. R. and Bass, A. H. (1998). Behavioral assessment of acoustic parameters relevant to signal recognition and preference in a vocal fish. *J. Acoust. Soc. Am.* **104**, 3520-3533.
McLean, D. L., Masino, M. A., Koh, I. Y., Lindquist, W. B. and Fetcho, J. R. (2008). Continuous shifts in the active set of spinal interneurons during changes in locomotor speed. *Nat. Neurosci.* **11**, 1419-1429.
Moulton, J. D. and Yan, Y. L. (2008). Using Morpholinos to control gene expression. *Curr. Protoc. Mol. Biol.*, chapter 26, unit 26.8.
Nicolson, T. (2005). The genetics of hearing and balance in zebrafish. *Annu. Rev. Genet.* **39**, 9-22.
Pitchford, S. and Ashmore, J. F. (1987). An electrical resonance in hair cells of the amphibian papilla of the frog *Rana temporaria*. *Hear. Res.* **27**, 75-83.
Popper, A. N. and Fay, R. R. (1993). Sound detection and processing by fish: critical review and major research questions. *Brain Behav. Evol.* **41**, 14-38.
Popper, A. N. and Fay, R. R. (2011). Rethinking sound detection by fishes. *Hear. Res.* **273**, 25-36.
Ramanathan, K., Michael, T. H., Jiang, G. J., Hiel, H. and Fuchs, P. A. (1999). A molecular mechanism for electrical tuning of cochlear hair cells. *Science* **283**, 215-217.
Rohmann, K. N. and Bass, A. H. (2011). Seasonal plasticity of auditory hair cell frequency sensitivity correlates with plasma steroid levels in vocal fish. *J. Exp. Biol.* **214**, 1931-1942.
Rohmann, K. N., Deitcher, D. L. and Bass, A. H. (2009). Calcium-activated potassium (BK) channels are encoded by duplicate slo1 genes in teleost fishes. *Mol. Biol. Evol.* **26**, 1509-1521.
Rohmann, K. N., Fergus, D. J. and Bass, A. H. (2013). Plasticity in ion channel expression underlies variation in hearing during reproductive cycles. *Curr. Biol.* **23**, 678-683.
Sausbier, M., Hu, H., Arntz, C., Feil, S., Kamm, S., Adelsberger, H., Sausbier, U., Sailer, C. A., Feil, R., Hofmann, F. et al. (2004). Cerebellar ataxia and Purkinje cell dysfunction caused by Ca^{2+}-activated K^{+} channel deficiency. *Proc. Natl. Acad. Sci. USA* **101**, 9474-9478.
Sisneros, J. A. (2009). Seasonal plasticity of auditory saccular sensitivity in the vocal plainfin midshipman fish, *Porichthys notatus*. *J. Neurophysiol.* **102**, 1121-1131.
Starr, C. J., Kappler, J. A., Chan, D. K., Kollmar, R. and Hudspeth, A. J. (2004). Mutation of the zebrafish choroideremia gene encoding Rab escort protein 1 devastates hair cells. *Proc. Natl. Acad. Sci. USA* **101**, 2572-2577.
Steinacker, A. and Romero, A. (1992). Voltage-gated potassium current and resonance in the toadfish saccular hair cell. *Brain Res.* **574**, 229-236.
Sugihara, I. and Furukawa, T. (1989). Morphological and functional aspects of two different types of hair cells in the goldfish sacculus. *J. Neurophysiol.* **62**, 1330-1343.
Tanimoto, M., Ota, Y., Horikawa, K. and Oda, Y. (2009). Auditory input to CNS is acquired coincidentally with development of inner ear after formation of functional afferent pathway in zebrafish. *J. Neurosci.* **29**, 2762-2767.
Westerfield, M. (2007). *The Zebrafish Book: A Guide for the Laboratory Use of Zebrafish (Danio rerio)*. Eugene, OR: University of Oregon Press.